JAERI-Research
2003-030

IONIZATION DYNAMICS OF A XENON ATOM IN SUPER-STRONG LASER FIELDS

December 2003

Koichi YAMAKAWA, Yutaka AKAHANE, Yuji FUKUDA
Makoto AOYAMA, Norihiro INOUE, Hideki UEDA
and Takayuki UTSUMI

日本原子力研究所
Japan Atomic Energy Research Institute

本レポートは，日本原子力研究所が不定期に公刊している研究報告書です。
入手の問合わせは，日本原子力研究所研究情報部研究情報課（〒319-1195　茨城県那珂郡東海村）あて，お申し越しください。なお，このほかに財団法人原子力弘済会資料センター（〒319-1195　茨城県那珂郡東海村日本原子力研究所内）で複写による実費頒布をおこなっております。

This report is issued irregularly.
Inquiries about availability of the reports should be addressed to Research Information Division, Department of Intellectual Resources, Japan Atomic Energy Research Institute, Tokai-mura, Naka-gun, Ibaraki-ken, 319-1195, Japan.

編集兼発行　　日本原子力研究所

JAERI-Research 2003-030

Ionization Dynamics of a Xenon Atom in Super-strong Laser Fields

Koichi YAMAKAWA, Yutaka AKAHANE, Yuji FUKUDA, Makoto AOYAMA,

Norihiro INOUE, Hideki UEDA, Takayuki UTSUMI

Advanced Photon Research Center

Kansai Research Establishment

Japan Atomic Energy Research Institute

Kizu-cho, Souraku-gun, Kyoto

(Received October 28, 2003)

We report on detailed investigations of ionization dynamics of a xenon atom exposed to intense 800-nm pulses of 20-fs duration in the extensive intensity range from 10^{13} to 10^{18} W/cm^2. Ion yields of Xe^+ to Xe^{20+} were observed as a function of laser intensity and compared with the results from a single active electron (SAE) based Ammosov-Delone-Krainov (ADK) model. Unexpected ionization probabilities for lower charge states and also no interplay between the inner- and outer-shells by screening are inferred. Suppression of nonsequential ionization towards higher intensity and few optical cycle regimes is also proved.

Keywords: T-cube Laser, Tunneling Ionization, Multiply Charged Ion, Rare Gas Atom, Relativistic Effect, Many Electron Atoms

超高強度レーザー場におけるキセノン原子のイオン化ダイナミクス

日本原子力研究所関西研究所光量子科学研究センター
山川　考一・赤羽　温・福田　祐仁・青山　誠
井上　典洋・上田　英樹・内海　隆行

（2003 年 10 月 28 日受理）

波長 800nm、パルス幅 20fs のレーザー光を集光強度 10^{13} W/cm^2 から 10^{18} W/cm^2 の範囲でキセノン原子に照射し、そのイオン化過程におけるダイナミクスについて研究を行った。レーザー照射強度に対するキセノン 1 価から 20 価イオンまでのイオン化収率を測定し、トンネルイオン化モデルとの比較を行った結果、(1) 低価数イオンにおける予想外なイオン化収率の向上、(2) 遮蔽効果による外殻と内殻電子群の非相互作用、(3) 相対論レーザー強度及び数サイクルパルスによる多電子同時イオン化の抑制、等が明らかとなった。これらの新しい発見は、このような高強度場において多電子原子がどのように振る舞うかを知る上で、新しい知見を与えるものである。

関西研究所：〒619-0215　京都府相楽郡木津町梅美台 8-1

Contents

目次

1. Introduction

The presence of strong laser fields radically alters the nature of atomic systems. Understanding the dynamical behavior of atoms exposed to external fields is fundamental to provide knowledge of properties of matter under such extreme conditions, as well as solutions to control new physical effects for many applications. Over the last two decades a large number of groups have studied the interaction of laser fields with atoms in the regime from multiphoton to tunneling ionization [1]. In the meantime, experimental measurements of the ion yields of various rare gas atoms have been performed as a function of laser intensity and compared with those predicted by several different theories in order to clarify the ionization dynamics of the atoms. For instance, highly charged ions up to Xe^{8+} have been produced by using a variety of laser systems, such as a 10-μm, 1-ns CO_2 laser [2], 1-μm, 1-ps Nd:glass laser [3], 0.8-μm, 200-fs Ti:sapphire laser [4], 0.586-μm, 1-ps dye laser [5], and 0.193- μm, 10-ps ArF* laser [6], respectively, with laser intensities of up to ~ 10^{16} W/cm^2. In the tunneling regime, the Ammosov-Delone-Krainov (ADK) model based on a quasi-classical tunneling theory provides a relatively good fit to sequential photoionization rates of the rare gas atoms [7]. In contrast, simultaneous tunneling of more than one electron (so called nonsequential or multi-electron ionization) shows experimentally that the production of doubly or multiply charged ions is more effective by many orders of magnitude than predicted by the ADK model [4, 8-10]. A number of models and numerical calculations have been applied [8, 11-15], but the explanation for this physical mechanism is still not known. Up to now, most of atomic physics is concerned with the behavior of valence electrons. Therefore, the quest for a many-electron problem of isolated atomic systems remains a distant goal for understanding the behavior of atoms exposed to strong laser fields.

Modern high-power lasers can now access to extraordinary high intensities of 10^{20} W/cm^2 in extremely short durations of 10-fs at unprecedented high repetition rates

of 36,000 shots per hour. Such super-strong fields correspond to 60 times the field binding the ground state electron in the hydrogen atom and inner shell electrons for heavy (high Z) atoms can't remain within the atomic center. At such intensities the electron velocity in the laser field also becomes relativistic. Thus, the free electrons move at close to the speed of light and their mass changes dramatically compared to their rest mass. Consequentially, it is now possible to test many-electron dynamics of complex atoms in radically new ways.

In this paper, we report on optical field ionization of a xenon atom by 800-nm, 10-Hz laser pulses of 20-fs duration with peak intensities ranging from 10^{13} to 10^{18} W/cm^2. The experiments reported herein exhibit three major findings. These are (1) unexpected ionization probabilities for lower charge states, also (2) no interplay between the inner- and outer-shells by screening, and (3) suppression of nonsequential ionization towards relativistic intensity and also few optical cycle regimes. These new findings have given us a hint of how many-electron systems behave in such fields.

2. Experiment

The present work uses a table-top, next generation of Ti:sapphire chirped-pulse amplification (CPA) system [16] that generates 100-TW, 20-fs, 10-Hz pulses with the capability of producing extremely highly-charged ions up to Ar^{16+}, Kr^{19+} and Xe^{26+}, respectively, at the laser intensity up to ~ 3 x 10^{19} W/cm^2. In order to clarify the ionization dynamics of the xenon atom, measurements of the ion yields as a function of the laser intensity were carried out with the signal-averaging technique at the intensity range from 10^{13} to 10^{18} W/cm^2. In our experiment, the linearly polarized laser light was focused using an off-axis parabolic mirror of focal length 161 mm in the center of the ionization chamber having a background pressure below 8 x 10^{-9} Torr. The xenon

pressure in the ionization chamber was controlled typically below 10^{-7} Torr in order to reduce space charge and collective effects. The maximum energy and pulse duration were measured to be 80-mJ and 20-fs, respectively. We obtained the focal spot diameter of 12 μm at $1/e^2$ with 74% of full energy, which corresponds to the estimated maximum intensity of ~ 6.0×10^{18} W/cm^2. The signal-to-background intensity contrast ratio was approximately 10^{-6} at a time scale of ± 2-ns. We used a half wave plate and polarizer to vary the intensity of the laser pulse. Both of them were placed after the Ti:sapphire amplifier and before the pulse compressor in order to eliminate accumulated B-integral and additional high-order dispersions after compression. Three sets of intensity scans were performed with a combination of different amplifier stages and partial reflection mirrors in the intensity range from (1) 6×10^{13} to 9×10^{15} W/cm^2, (2) 6×10^{14} to 1.5×10^{17} W/cm^2, and (3) 1×10^{17} to 1.5×10^{18} W/cm^2, respectively. The ion species are separated with a 1-m time-of-flight (TOF) mass spectrometer and detected with dual micro channel plates. An adjustable slit with a width of 300 μm is placed between the acceleration grids and MCP detector on the central axis of the flight tube in order to detect the ions produced in the highest intensity focal region while eliminating the background noise produced by ionizing contaminants in the large focal volume and low-intensity region. A further subtraction of the volume effects was performed by considering integration over a region which is limited by the slit [4]. Each data run consists of 1,000 laser shots with the laser energy-fluctuations of less than 5%, which was not accessible by using the large-scale, single-shot per hour, high-intensity Nd:glass CPA lasers.

The results of the ion-yield data for xenon as a function of laser intensity are shown in Fig. 1. The theoretical curves calculated by the ADK model are also shown as the references in this figure. In this model, only sequential (stepwise) ionization has been considered. It should be noted that all the charge states were produced in the regime of $\gamma < 1$ (Keldysh γ parameter) [17] except for Xe^+ ($\gamma \cong 1$), which indicated we

performed the experiment exclusively in the tunneling regime. The results presented in Fig. 1 clearly show disagreement between the experimental ion curves and those from the ADK model along the laser intensity scale. In order to compare between the experimental ion curves and those obtained theoretically, we evaluate a shift factor on each ion curve along the intensity scale by the least-squares method. The shift factor is listed in Table 1. The shift factor listed here is the number by which the theoretical intensity scales have been multiplied. For example, a factor of 0.7 means that the theoretical curve for that charge state is shifted lower in intensity by 30%. The experimental curve of Xe^{2+} already begins to disagree with the theoretical one by 15%, while a comparison between the experimental curves of Xe^{3+} to Xe^{6+} and those from the ADK model shows rather poor agreement. For example, the experimental curve of Xe^{4+} disagrees with the theoretical one by nearly 50%. We emphasize that we repeated the measurements for several times and saw no discernible shifts in the *relative* positions of all the ion yields data, which means that the disagreements are due to some physical differences in the ionization processes [18]. It should be also pointed out that most of the previous reports focus on finding the knee structure (which is also discussed later on), which is the deviation from the sequential ADK tunneling ionization model at the laser intensities below ionization saturation. However, in the cases of Xe^{3+} to Xe^{6+}, for example, our experimental data completely disagree with the calculated curves even in the saturation intensity regions.

3. Discussion

In general, the atomic ionization energy is a unique and fundamental property for all elements. However, high-precision determinations of the ionization energy, especially for complex atoms are relatively rare. Even though, the factors of 0.5-0.7 for Xe^{3+} to Xe^{6+} completely deviated from the measurement accuracy of the ionization

energy mentioned above. Therefore, the influence of the many-electron dynamics in the strong laser field should not be neglected. More surprisingly, the experimental curve for Xe^{9+} returns to fit the theoretical one subsequently ejecting all the electrons from the n = 5 shell of xenon. This result indicates the absence of a relationship between the 4d inner shell and the n = 5 outer shell. Therefore, we may emphasize that the ionization processes strongly depend on the atomic structure and outermost shell density.

So far, a small amount of theoretical work has been carried out to test the dynamics and interplay of outer and inner shells in complex atoms. Boyer and Rhodes [19], and Szöke and Rhodes [20] have suggested that the 4d inner shell state of xenon can be strongly excited by coherently driven 5p shell electrons. In contrast, L'Huillier et al. have shown that the 4d inner shell will be shielded from the external field by the outer 5p shell [21]. In the later case, multiple ionization in the n =5 shell, therefore, varies by screening effects. For a given external laser intensity, the effective (local) intensity should increase for each step of the stripping process by screening, increasing the probability for creation of higher charge states. This is what we observe in the experimental ion curves towards lower intensities. Considering the result in the case of Xe^{9+}, it is also favorable to the case suggested by L'Huillier et al. It is simply explained as follows. Stripping of the outer shell occurs by the leading edge of the pulse, which reduces the screening. The effective intensity in the 4d inner shell then approaches the given external intensity and leads to sequential tunneling ionization. As for the charge state of Xe^{19+}, the experimental curve differs from the theoretical one by 15%. Although the transition from the 4d to 4p sub-shells (ionization potentials from 452 eV to 549 eV) [22] are relatively large, it might be possible for the existence of some coupling mechanisms among these electrons in those sub-shells as they are more tightly bound. There should be a limit to apply their analysis in our experimental regime since it is only based on the framework of the perturbation theory. However it is difficult to

make a general statement at the moment, because it will probably take quite some time for the theory to provide reasonably systematic description of the role of implications of many-electrons in strong and super-strong laser fields. Our observation should aid in distinguishing between the viability of future models.

As part of the comparison between the experimental curves and those obtained theoretically, we shift the theoretical ones along the laser intensity scale to match the data in order to look at the presence of the knee structures described previously. This is presented in Fig. 2 and made based on the shift factor listed in Table 1. From Fig. 2, it is clear that the experimental ion yields of Xe^{2+} to Xe^{7+} are more effective by orders of magnitude than predicted by the ADK model at the laser intensities below saturation of ionizations while the ion yields of Xe^{8+} to Xe^{20+} can be thought to follow the calculations. The discrepancies in Xe^{2+}- Xe^{7+} yields between the experiment and the ADK model at these intensities are a signature of NS ionization.

To compare our result with the previous ones by other groups, we refer the most suitable experiment for six-fold ionizations of xenon with a femtosecond Ti:sapphire laser pulse [4]. The experimental data presented in Ref. 4 have been also compared with the results [23] of the correlated energy sharing model, based on the so called "intense-field many-body S-matrix theory" (IMST) [14]. In this model an active electron first absorbs the photon energy from the laser field by virtual above-threshold ionization, and then shares this energy with the other N-electrons via the electron correlation, until they have enough energy to escape together from the nucleus. The calculated results for the ion yields of the charge states up to Xe^{6+} were found to agree remarkably well with the measured ones. Considering the situation of our results, we first found that the ionization threshold intensities for the data presented here are in most cases much higher than seen in Ref. 23. As far as we know, the duration of the pulse at a given peak intensity does influence the final outcome of ionization. The experiment

described in Ref. 4 was performed with a 200 fs-duration (~ 80 optical cycles), 800-nm pulse, whereas the experiment described here used 20-fs duration (~ 8 optical cycles), 800-nm pulse. Perhaps the most interesting effect is the shift of the saturation intensity to higher values as the pulse becomes shorter. As a result, some of the ionic species (especially those of lower q) are exposed to somewhat higher intensity. The production of higher charged ions, on the other hand, does not seem to be affected much by this change of the pulse duration, the main reason being that the higher charged ions are produced mostly during the short interval of high intensity even for the long pulse. As a consequence of this shift of saturation intensities, it is observed that the range of peak intensities in which most of the ionization occurs has narrowed as the pulse duration became shorter.

The total probability of NS ionization seems to also depend on the pulse duration. The rescattering model [11] is a model in which the outer electron is promoted into the continuum and then driven by the oscillating laser field, and the electron returns and interacts with the parent ion, where it can ionize the second electron. In this manner the NS ionization yield depends on the number of returns of the electron and, therefore, on the number of optical cycles of the laser pulse [24]. Our result seems to be consistent with the model, since the total probabilities of NS ionization for Xe^{2+} to Xe^{7+} were much lower than seen in Ref. 23.

Although the IMST calculation of the ion yields for the charge states higher than Xe^{8+} has not yet been performed so far, from a classical point of view, the tendency of the ionic charge state yields of over Xe^{9+} can be qualitatively explained by suppression of NS ionization with increasing laser intensities towards the relativistic regime [25]. The ponderomotive energy of the free electron is on the order of 0.1 MeV at a laser intensity of ~ 10^{18} W/cm^2 and therefore the electron velocity becomes relativistic. In this case the magnetic field component is no longer negligible, causing a forward drift

momentum of photoelectrons in the laser propagation direction. It means that the Lorentz force in this super-strong field may reduce rescattering of laser-driven electrons. For example, a result of a classical trajectory of the ionized electron by our one-dimensional calculation shows that the displacement of the electron along to the laser propagation direction is of the order of 10-nm over the half laser cycle at the laser intensity of 10^{17} W/cm^2. Then, the electron loses the parent ion and no rescattering will occur. Our experimental result, therefore, confirms the indirect evidence for the suppression of NS ionization of Xe at the *fixed* relativistic laser intensity [26]. As for the charge state of Xe^{8+} at the laser intensity of around 10^{16} W/cm^2, however, the magnetic field component at this intensity seems to be not strong enough to induce the displacement of the returning electrons (on the order of a few angstroms over the half laser cycle). Consequently, the suppression of NS ionization for Xe^{8+} and certainly higher ones is also probably due to the small core size with the decrease in the inelastic scattering cross section as well as the reduction of the laser optical cycles mentioned previously.

4. Conclusion

We have studied the interaction of strong laser fields with the xenon atom, spanning the peak intensity range from 10^{13} to 10^{18} W/cm^2. It is concluded that the conventional treatments of multiple ionization do not correspond to our experimental findings for the many-electron atom. The essential findings were (1) unexpected ionization probabilities for lower charge states, also (2) no interplay between the inner- and outer-shells by screening, and (3) suppression of nonsequential ionization towards relativistic intensity and also few optical cycle regimes. These new findings have given us a hint of how many-electron systems behave in such fields. A further study of the interaction of radiation with various complex atoms under these extreme conditions

provides knowledge of the fundamental properties of matter, as well as solutions to control these new physical effects for potential applications, such as the generation of Larmor radiation [27] and x-ray laser [28], ultrahigh-order harmonic generation [29], and particle acceleration [30]. Oncoming theoretical predictions for all these investigations presented here will help to further understand new insight into atomic dynamics. At last, a quantitative theory of relativistic ionization of hydrogen-like ions is being approached recently [31].

Acknowledgements.

The authors acknowledge C. H. Keitel and F. H. M. Faisal for fruitful discussions in the early stage of this work. They also thank T. Kimura, T. Tajima, and Y. Kato for their encouragement.

References

1. See for example, *Multiphoton Processes*, edited by L. F. DiMauro, R. R. Freeman, K. C. Kulander, AIP Conf. Proc. No. 525 (AIP, New York, 2000).
2. S. L. Chin, W. Xiong, P. Lavigne, J. Opt. Soc. Am. B **4**,853 (1987).
3. S. Augst, *et al.* Phys. Rev. Lett. **63**, 2212 (1989).
4. S. Larochelle, A. Talebpour, S. L. Chin, J. Phys. B **73**, 1201 (1998).
5. M. D. Perry, *et al.* Phys. Rev. Lett. **60**, 1270 (1988).
6. T. S. Luk, *et al.* Phys. Rev. Lett. **51**, 110 (1983).
7. M. V. Ammosov, N. B. Delone, V. P. Krainov, Sov. Phys. JETP **64**, 1191 (1986).
8. D. N. Fittinghoff, *et al.* Phys. Rev. Lett. **69**, 2642 (1992).
9. B. Walker, *et al.* Phys. Rev. Lett. **73**, 1227 (1994).
10. Th. Weber, *et al. Nature* **405**, 658 (2000).
11. P. B. Corkum, Phys. Rev. Lett. **73**, 1994 (1993).
12. J. B. Watson, *et al.* Phys. Rev. Lett. **78**, 1884 (1997).
13. K. T. Taylor, *et al.* Laser Phys. **9**, 98 (1999).
14. A. Becker, F. H. M. Faisal, Phys. Rev. A **59**, R1742 (1999).
15. U. Eichmann, *et al.* Phys. Rev. Lett. **84**, 3550 (2000).
16. K. Yamakawa, *et al.* Opt. Lett. **23**, 1468 (1998).
17. L. V. Keldysh, Sov. Phys. JETP **20**, 1307 (1965).
18. We have also obtained good agreement between the experimental ion curves and those from the ADK model for lower charge states of Ar and Kr with no shift in laser intensity scale.
19. K. Boyer, C. K. Rhodes, Phys. Rev. Lett. **54,** 1490 (1985).

20. A. Szöke, C. K. Rhodes, Phys. Rev. Lett. **56,** 720 (1986).

21. A. L'Huillier, L. Jönsson, G. Wendin, Phys. Rev.A. **33,** 3938 (1986).

22. R. D. Cowan, *The Theory of Atomic Structure and Spectra* (The University California Press, California, 1981)

23. A. Becker, & F. H. M. Faisal, Phys. Rev. A **59**, R3182 (1999).

24. V. R. Bhardwaj, *et al.* Phys. Rev. Lett. **86**, 3522 (2001).

25. C. H. Keitel, P. L. Knight, Phys. Rev. A **51**, 1420 (1995).

26. M. Dammasch, *et al.* Phys. Rev. A **64**, 061402(R) (2001).

27. Y. Ueshima, *et al.* Laser & Particle Beams **17**, 45 (1999).

28. A. McPherson, *et al.* Nature **370**, 631 (1994).

29. D. B. Milosevic, S. Hu, & W. Becker, Phys. Rev. A **63**, 011403(R) (2001).

30. T. Tajima, J. M. Dawson, Phys. Rev. Lett. **43**, 267 (1979).

31. N. Milosevic, V. P. Krainov, T. Brabec, Phys. Rev. Lett. **89**, 193001-1 (2002).

Table. 1 Shift in theoretical curves needed to match experimental data. Shift in theoretical curves needed to match experimental data. The shift factor listed here is the number by which the theoretical intensity scales have been multiplied. For example, a factor of 0.7 means that the theoretical curve for that charge state is shifted lower in intensity by 30%.

Energy level	Charge state	Ionization energy (eV) [22]	Shift factor
5p	1	12.13	1.00
	2	21.21	0.85
	3	32.1	0.70
	4	46.7	0.55
	5	59.7	0.60
	6	71.8	0. 75
5s	7	92.1	0.90
	8	105.9	0.80
4d	9	171	0.95
	10	202	1.00
	11	233	0.90
	12	263	0.85
	13	294	0.80
	14	325	0.85
	15	358	0.80
	16	390	0.80
	17	421	1.00
	18	452	0.90
4p	19	549	0.85
	20	583	0.95

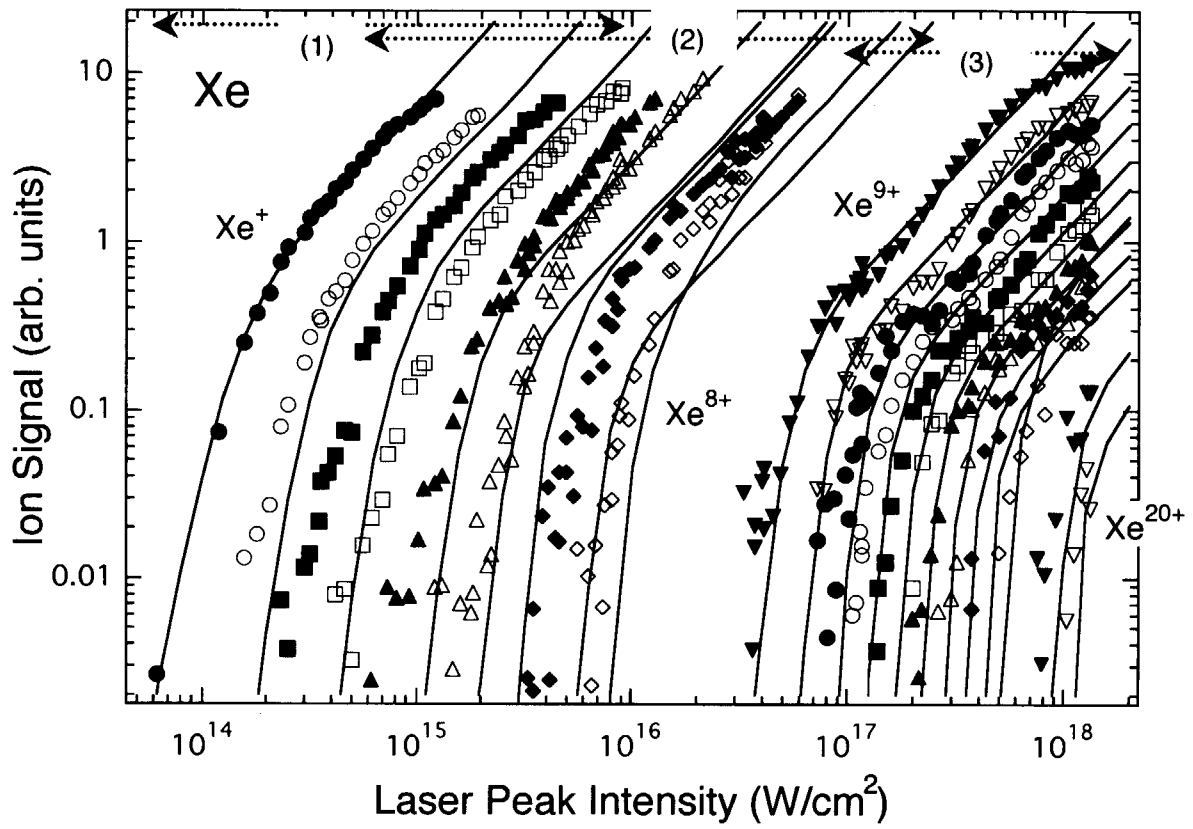

Fig. 1 Comparison of experiment and theory for tunneling ionizations in Xe as a function of laser intensity. Experiment: λ = 800-nm, τ = 20-fs, Theory: the quasi-classical tunneling theory (solid curves) with no shift in laser intensity. Three sets of intensity scans; (1) 6 x 10^{13} to 9 x 10^{15} W/cm^2, (2) 6 x 10^{14} to 1.5 x 10^{17} W/cm^2, and (3) 1 x 10^{17} to 1.5 x 10^{18} W/cm^2, are indicated.

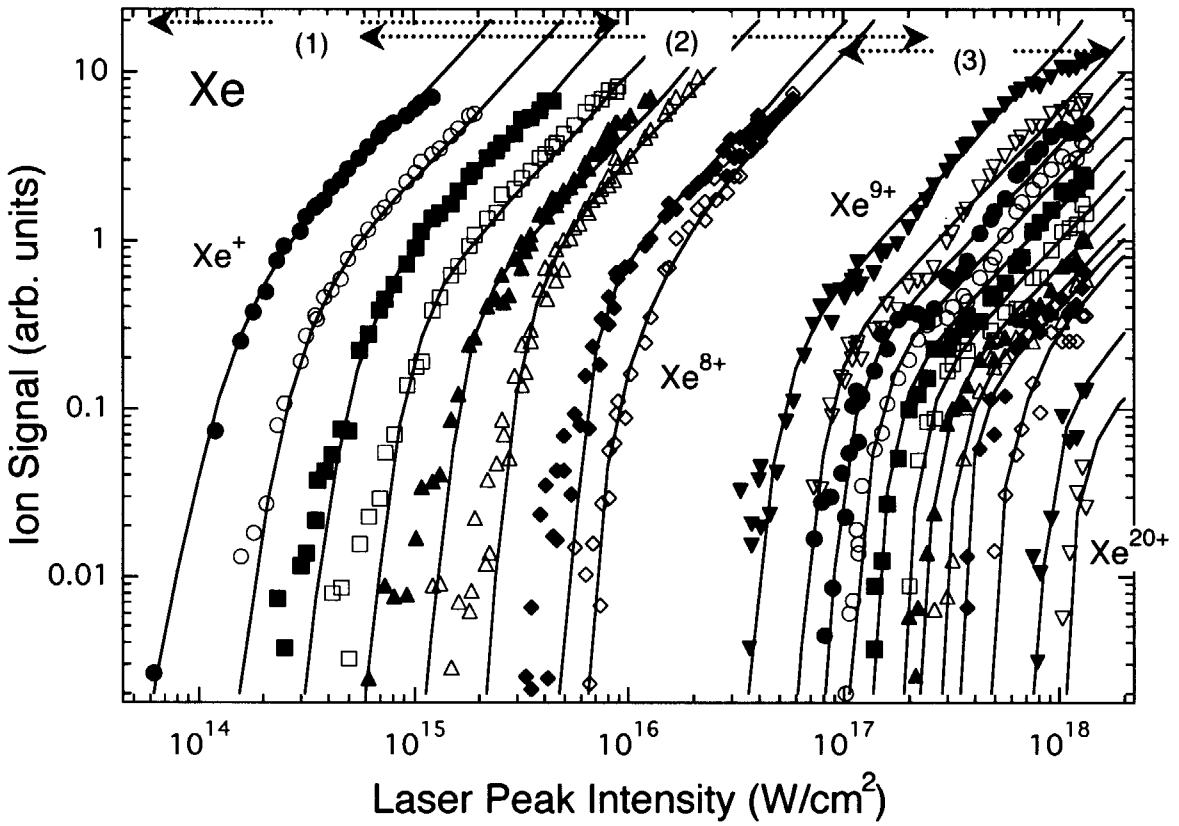

Fig. 2 Comparison of experiment and theory for tunneling ionizations in Xe as a function of laser intensity that is identical to Fig. 1, but with shift the theoretical curves along the laser intensity scale to match the experimental data. The solid curves (theory) represent the "best fit" to the data based on the shift factor listed in Table 1.

国際単位系（SI）と換算表

表1　SI基本単位および補助単位

量	名称	記号
長さ	メートル	m
質量	キログラム	kg
時間	秒	s
電流	アンペア	A
熱力学温度	ケルビン	K
物質量	モル	mol
光度	カンデラ	cd
平面角	ラジアン	rad
立体角	ステラジアン	sr

表2　SIと併用される単位

名称	記号
分，時，日	min, h, d
度，分，秒	°, ′, ″
リットル	l, L
トン	t
電子ボルト	eV
原子質量単位	u

1 eV=1.60218×10^{-19}J

1 u=1.66054×10^{-27}kg

表3　固有の名称をもつSI組立単位

量	名称	記号	他のSI単位による表現
周波数	ヘルツ	Hz	s^{-1}
力	ニュートン	N	$m\cdot kg/s^2$
圧力，応力	パスカル	Pa	N/m^2
エネルギー,仕事,熱量	ジュール	J	N·m
工率，放射束	ワット	W	J/s
電気量，電荷	クーロン	C	A·s
電位，電圧，起電力	ボルト	V	W/A
静電容量	ファラド	F	C/V
電気抵抗	オーム	Ω	V/A
コンダクタンス	ジーメンス	S	A/V
磁束	ウェーバ	Wb	V·s
磁束密度	テスラ	T	Wb/m^2
インダクタンス	ヘンリー	H	Wb/A
セルシウス温度	セルシウス度	℃	
光束	ルーメン	lm	cd·sr
照度	ルクス	lx	lm/m^2
放射能	ベクレル	Bq	s^{-1}
吸収線量	グレイ	Gy	J/kg
線量等量	シーベルト	Sv	J/kg

表4　SIと共に暫定的に維持される単位

名称	記号
オングストローム	Å
バーン	b
バール	bar
ガル	Gal
キュリー	Ci
レントゲン	R
ラド	rad
レム	rem

1 Å=0.1nm=10^{-10}m

1 b=100fm^2=10^{-28}m^2

1 bar=0.1MPa=10^{5}Pa

1 Gal=1cm/s^2=10^{-2}m/s^2

1 Ci=3.7×10^{10}Bq

1 R=2.58×10^{-4}C/kg

1 rad=1cGy=10^{-2}Gy

1 rem=1cSv=10^{-2}Sv

表5　SI接頭語

倍数	接頭語	記号
10^{18}	エクサ	E
10^{15}	ペタ	P
10^{12}	テラ	T
10^{9}	ギガ	G
10^{6}	メガ	M
10^{3}	キロ	k
10^{2}	ヘクト	h
10^{1}	デカ	da
10^{-1}	デシ	d
10^{-2}	センチ	c
10^{-3}	ミリ	m
10^{-6}	マイクロ	μ
10^{-9}	ナノ	n
10^{-12}	ピコ	p
10^{-15}	フェムト	f
10^{-18}	アト	a

（注）

1．表1－5は「国際単位系」第5版，国際度量衡局1985年刊行による。ただし，1 eVおよび1 uの値はCODATAの1986年推奨値によった。

2．表4には海里，ノット，アール，ヘクタールも含まれているが日常の単位なのでここでは省略した。

3．barは，JISでは流体の圧力を表わす場合に限り表2のカテゴリーに分類されている。

4．EC閣僚理事会指令ではbar，barnおよび「血圧の単位」mmHgを表2のカテゴリーに入れている。

換算表

力	N(=10^{5}dyn)	kgf	lbf
	1	0.101972	0.224809
	9.80665	1	2.20462
	4.44822	0.453592	1

粘度　1 Pa·s(N·s/m^2)=10 P(ポアズ)(g/(cm·s))

動粘度　1m^2/s=10^{4}St(ストークス)(cm^2/s)

圧力	MPa(=10bar)	kgf/cm^2	atm	mmHg(Torr)	lbf/in^2(psi)
	1	10.1972	9.86923	7.50062×10^3	145.038
	0.0980665	1	0.967841	735.559	14.2233
	0.101325	1.03323	1	760	14.6959
	1.33322×10^{-4}	1.35951×10^{-3}	1.31579×10^{-3}	1	1.93368×10^{-2}
	6.89476×10^{-3}	7.03070×10^{-2}	6.80460×10^{-2}	51.7149	1

エネルギー・仕事・熱量	J(=10^7 erg)	kgf·m	kW·h	cal(計量法)	Btu	ft·lbf	eV
	1	0.101972	2.77778×10^{-7}	0.238889	9.47813×10^{-4}	0.737562	6.24150×10^{18}
	9.80665	1	2.72407×10^{-6}	2.34270	9.29487×10^{-3}	7.23301	6.12082×10^{19}
	3.6×10^6	3.67098×10^5	1	8.59999×10^5	3412.13	2.65522×10^6	2.24694×10^{25}
	4.18605	0.426858	1.16279×10^{-6}	1	3.96759×10^{-3}	3.08747	2.61272×10^{19}
	1055.06	107.586	2.93072×10^{-4}	252.042	1	778.172	6.58515×10^{21}
	1.35582	0.138255	3.76616×10^{-7}	0.323890	1.28506×10^{-3}	1	8.46233×10^{18}
	1.60218×10^{-19}	1.63377×10^{-20}	4.45050×10^{-26}	3.82743×10^{-20}	1.51857×10^{-22}	1.18171×10^{-19}	1

1 cal= 4.18605J（計量法）

= 4.184J（熱化学）

= 4.1855J（15℃）

= 4.1868J（国際蒸気表）

仕事率　1 PS(仏馬力)

= 75 kgf·m/s

= 735.499W

放射能	Bq	Ci
	1	2.70270×10^{-11}
	3.7×10^{10}	1

吸収線量	Gy	rad
	1	100
	0.01	1

照射線量	C/kg	R
	1	3876
	2.58×10^{-4}	1

線量当量	Sv	rem
	1	100
	0.01	1

（86年12月26日現在）

Ionization Dynamics of a Xenon Atom in Super-strong Laser Fields